UNIVERSITY
of
GLASGOW

Department of Physics & Astronomy
Experimental Particle Physics Group
Kelvin Building, University of Glasgow,
Glasgow, G12 8QQ, Scotland
Telephone: +44 (0)141 339 8855 Fax: +44 (0)141 330 5881

GLAS-PPE/2009-04
16th June 2009

Two-Body Charmless Baryonic B Decays at LHCb

Laurence Carson[1], Eduardo Rodrigues[1]

[1]Department of Physics and Astronomy, University of Glasgow,
Glasgow, G12 8QQ

Abstract

The potential of the LHCb experiment to make the first discovery of a two-body charmless baryonic B decay is explored. The most promising channel is $B^0 \to p\bar{p}$, for which a 5σ discovery is possible with around 0.25 fb^{-1} of LHCb data at nominal centre-of-mass energy, assuming that the value for the $B^0 \to p\bar{p}$ branching ratio is close to the current experimental upper limit. LHCb also has prospects for other two-body charmless baryonic B decays, such as $B_s \to p\bar{p}$ and decays involving a Λ.

Contents

1 Introduction

The observation of B meson decays into two light (charmless) mesons has been made in several decay modes. But despite searches with the CLEO detector and at the SLAC and KEK B-factories, no charmless two-body baryonic B decay has yet been observed [1, 2, 3]. This situation is in contrast with the observation of a multitude of three-body baryonic B decays. Empirically, the suppression of two-body compared to three-body baryonic B decays is well established; well-known examples are ($\mathscr{B}$ stands for the branching ratio):

$$\mathscr{B}(B^- \to p\bar{p}K^-) \gg \mathscr{B}(\bar{B}^0 \to p\bar{p})$$
$$\mathscr{B}(B^- \to \Lambda_c^+ \bar{p}\pi^-) \gg \mathscr{B}(\bar{B}^0 \to \Lambda_c^+ \bar{p})$$

Assuming a suppression factor in charmless decays (first example) similar to that observed in $b \to c$ transitions (second example), of order 0.1, the simplest two-body baryonic B decay, $B^0 \to p\bar{p}$, may be expected to have a branching ratio of order 10^{-7}, and therefore be observable at LHCb.

Theoretical predictions of the branching ratios for such two-body baryonic decays within the Standard Model (SM) vary depending on the method of calculation used. However, the predicted branching ratios are normally of order 10^{-6} or lower. The LHCb experiment [4, 5] is very well placed to make an observation of these rare decays, thanks to its excellent vertexing and particle identification (PID) abilities, which enable background to be suppressed while efficiently retaining signal events.

This note will concentrate on the particular channel $B^0 \to p\bar{p}$, which is topologically identical to decays such as $B_d \to \pi^+\pi^-$ and $B_s \to K^+K^-$, which have been the subject of much study within LHCb; the latter decays are referred to as $B \to h^+h^{'-}$ channels.

In section 2, the theoretical predictions for the SM branching ratios of relevant two-body charmless baryonic B decays will be summarised, along with the current best experimental upper limits on these branching ratios. The following two sections describe the selection of $B^0 \to p\bar{p}$ events and the possible sources of background. In section 5, the performance of the selection is given, along with the resulting background-to-signal ratios and signal significance as a function of the $B^0 \to p\bar{p}$ branching fraction. Section 6 lays out the strategy for measuring the $B^0 \to p\bar{p}$ branching ratio once a clear signal has been seen. Trigger mass window issues for $B^0 \to p\bar{p}$ are considered in section 7. In section 8, the prospects for the observation of other two-body charmless baryonic B decays are briefly discussed. Conclusions are given in section 9.

2 Current Status of Theory and Experiment

2.1 Theoretical Predictions for Branching Ratios

A theoretical calculation of the branching ratio for B meson decays involving baryons is challenging: the final state involves six quarks (rather than four as in a decay to two mesons), and the amplitudes typically require the production of a quark-antiquark pair out of the vacuum. This involves recoil effects which are not yet fully understood and hence are difficult to account for. The decay amplitudes are non-factorisable, and hence more difficult to evaluate.

The dominant decay amplitude for $B^0 \to p\bar{p}$ is expected to be the $b \to u$ tree-level process. This process is shown in Fig. 1. The penguin contribution may also play a role. Other possible diagrams such as annihilation, penguin annihilation and electroweak penguin processes can also contribute, but should have a rather small influence.

Predictions have been published using several different approaches. A summary of predictions using three different frameworks – QCD sum rules [6], diquark model [7] and pole model [8, 9] – is given in Tab. 1. It can be seen that the different theoretical approaches do not agree in their predictions, even in order of magnitude.

Note that within the pole model framework two different methods of calculating the hadronic matrix element are used: the harmonic oscillator model [8], and the MIT bag model [9]. The MIT bag model calculations only take the parity-conserving matrix element into account, as calculating the parity-violating matrix element in the bag model poses some additional theoretical challenges. The values presented in the table for the bag model are the parity-conserving-only values.

2.2 Experimental Limits on Branching Ratios

Charmless two-body baryonic B decays have been searched for by the CLEO experiment [10] at the Cornell storage ring, and by the B-factory experiments Babar [11] at the SLAC laboratory in California and Belle [12]

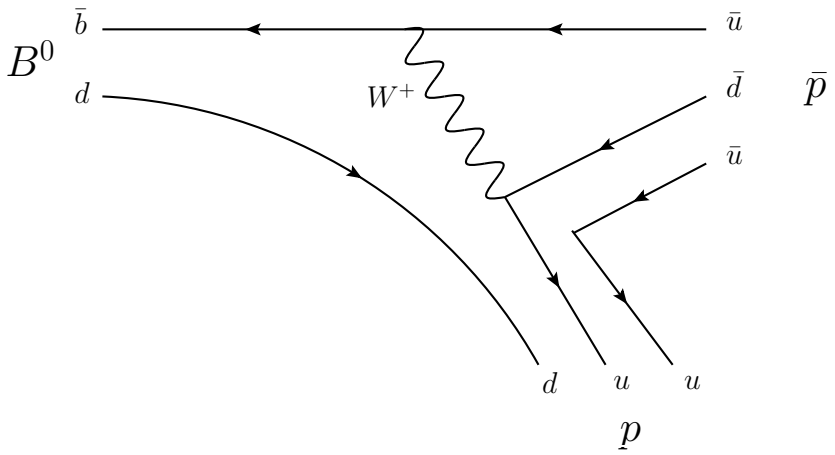

Figure 1: Feynman diagram for the tree-level process contributing to $B^0 \to p\bar{p}$.

Decay Channel	QCD Sum Rules	Diquark Model	Pole Model	
			Harmonic Oscillator Model	MIT Bag Model
$B^0 \to p\bar{p}$	1.2×10^{-6}	2.9×10^{-6}	7.0×10^{-6}	1.1×10^{-7}
$B^0 \to \Lambda\bar{\Lambda}$			2×10^{-7}	0
$B^+ \to p\bar{\Lambda}$	$\lesssim 3 \times 10^{-6}$			2.2×10^{-7}

Table 1: Theoretical predictions for the branching ratios of different baryonic two-body B decays. A blank entry indicates that the branching ratio was not calculated using that particular model.

at the KEK laboratory in Japan. Their current best upper limits on the branching ratios of several baryonic modes are listed in Tab. 2; they are of the order of 10^{-7}.

Decay Channel	Belle UL [1]	Babar UL [2]	CLEO UL [3]
$B^0 \to p\bar{p}$	1.1×10^{-7}	2.7×10^{-7}	7.0×10^{-6}
$B^0 \to \Lambda\bar{\Lambda}$	3.2×10^{-7}		3.9×10^{-6}
$B^+ \to p\bar{\Lambda}$	3.2×10^{-7}		2.6×10^{-6}

Table 2: Experimental upper limits on the branching ratios of different two-body charmless baryonic B decays. Limits shown correspond to a 90% confidence level.

The experimental 90% confidence level (C.L.) upper limit for the $B^0 \to p\bar{p}$ branching ratio, 1.1×10^{-7}, is dominated by the latest Belle search [1], which uses 414 fb^{-1} of data. It is interesting to note that this result has already ruled out the predictions of the QCD sum rules and diquark models, as well as the harmonic oscillator method within the pole model. Also pressure is starting to be applied to the prediction of the MIT bag model in the pole model. Updated results from Belle with a larger data sample – to date Belle has accumulated over 700 fb^{-1} at the $\Upsilon(4S)$ resonance – have the potential to exclude all theoretical calculations to date.

Considering the inconsistency among the several theoretical predictions for the $B^0 \to p\bar{p}$ branching ratio and the experimental data, it is clear that an early measurement of this branching ratio by LHCb could have an impact on the theoretical understanding of the dynamics involved in (two-body) baryonic B decays, while providing the first observation of a charmless two-body baryonic B decay.

3 Selection of $B^0 \to p\bar{p}$ Events

The decay $B^0 \to p\bar{p}$ is topologically identical to the $B \to h^+h'^-$ modes (where $h = K, \pi$) considered as core channels for the LHCb physics programme; their selection study is detailed in [13]. The set of cut variables optimised for the selection of the "standard" $B \to h^+h'^-$ decays served as a starting point for the selection

of $B^0 \to p\bar{p}$ candidates. Indeed, since that set of cuts efficiently selects signal events in these channels while keeping background from so-called $b\bar{b}$ inclusive (*i.e.* generic b-decays) and minimum bias events down to an acceptable level, it is reasonable to expect that it will perform well also for $B^0 \to p\bar{p}$ events.

To reduce the background level further, several extra cuts have been added to the $B \to h^+h^{'-}$ selection given in [13]. To select protons and reject charged pions and kaons, particle identification (PID) cuts on the difference between the log likelihood of two particle hypotheses, $\mathrm{DLL}(p-\pi) > 5$ and $\mathrm{DLL}(p-K) > 0$, were employed. A tighter proton-pion separation cut $\mathrm{DLL}(p-\pi)$ is necessary as a typical event contains more pions than kaons. In addition, a cut on the track quality, $\chi^2/n_{\mathrm{DoF}} < 3$, was applied to each of the daughter tracks in order to reduce the background due to ghost (fake) tracks.

The complete set of selection cuts (the standard selection plus the extra cuts as described above) is summarised in Tab. 3.

Type of cut	Value
B invariant mass window	± 50 MeV
Max. χ^2 of B vertex	5.0
Min. p_T of B	1.0 GeV
Max. IPS of B	2.5
Min. FDS of B	18.0
Min. p_T for both daughters	1.0 GeV
Min. p_T for (at least) one daughter	3.0 GeV
Min. IPS for both daughters	6.0
Min. IPS for (at least) one daughter	12.0
Min. $\mathrm{DLL}(p-\pi)$ for both daughters	5.0
Min. $\mathrm{DLL}(p-K)$ for both daughters	0.0
Max. number of tracks within 3σ of B vertex	15
Max. χ^2/n_{DoF} for both daughter tracks	3.0

Table 3: List of cuts applied in the selection of $B^0 \to p\bar{p}$ events. Note that p_T refers to transverse momentum, IPS refers to impact parameter significance, and FDS refers to flight distance significance.

4 Background studies

4.1 Sources of Background

As stated in Sec. 3, the $B \to h^+h^{'-}$ selection found in [13] enables high suppression of background from $b\bar{b}$ inclusive and minimum bias events. This leads to an expectation that the selection described above should suppress such backgrounds similarly well for $B^0 \to p\bar{p}$ events. Particular care is nevertheless needed, given the low $B^0 \to p\bar{p}$ branching ratio.

In addition to these inclusive backgrounds, two other potential sources of background were investigated: background from misidentified $B \to h^+h^{'-}$ final states or partially reconstructed three-body $B \to hhh$ decays.

Given their same signature and considerably higher branching ratios, $B \to h^+h^{'-}$ decays are a potentially dangerous source of background. We have considered the following decay modes: $B^0 \to K^+\pi^-$, $B_s \to K^+K^-$ and $\Lambda_b \to pK^-$. These are the higher branching ratio ($\approx 10^{-6} - 10^{-5}$) $B \to h^+h^{'-}$ channels which are likely to contribute most to the specific $B \to h^+h^{'-}$ background.

Partially reconstructed $B \to hhh$ decays are typically not a dangerous source of background in the analysis of the standard $B \to h^+h^{'-}$ modes because their reconstructed mass tends to fall significantly below the signal mass peak, as one track is not reconstructed. However, in the present analysis these decays have the potential to populate the $B^0 \to p\bar{p}$ mass peak region as the reconstructed mass of most two-track pairs from these decays will shift significantly upward under a proton mass hypothesis. The $B \to hhh$ decays considered in the present study are: $B^0 \to \pi^+\pi^-\pi^0$, $B^0 \to K_s\pi^-\pi^+$, $B^+ \to \pi^+\pi^-\pi^+$, $B^+ \to \pi^+\pi^-K^+$, $B^+ \to \pi^+K^-K^+$, $B^+ \to p\bar{p}\pi^+$, $B^+ \to p\bar{p}K^+$ and $B^+ \to K^+K^-K^+$.

4.2 Background Suppression

To examine the role of PID and invariant mass cuts in reducing the specific background, the invariant mass distributions for signal and background before applying PID cuts can be compared with those after the PID cuts are applied. The following four figures, Figs. 2-5, show the signal and specific background events from

2 fb^{-1} of data which are expected to pass the standard $B \to h^+h'^-$ selection with a very wide mass window of $m_{B^0} \pm 1200$MeV. On each figure, the left-hand plot shows the distributions before any PID cuts, and the right-hand plot shows the distributions after the application of the PID cuts given in Sec. 3. Note that the efficiency of these PID cuts on the signal is 73%.

Figure 2 shows the mass distribution for $B^0 \to p\bar{p}$ alongside those for the $B \to h^+h'^-$ channels considered as backgrounds here. Fig. 3 shows the mass distribution for $B^0 \to p\bar{p}$ alongside those for $B \to hhh$ channels where the reconstructed mass tends to fall well below m_{B^0}. Finally, Figs. 4 and 5 compare the signal mass distribution with those for the $B \to hhh$ channels where the reconstructed mass distribution overlaps significantly with the signal.

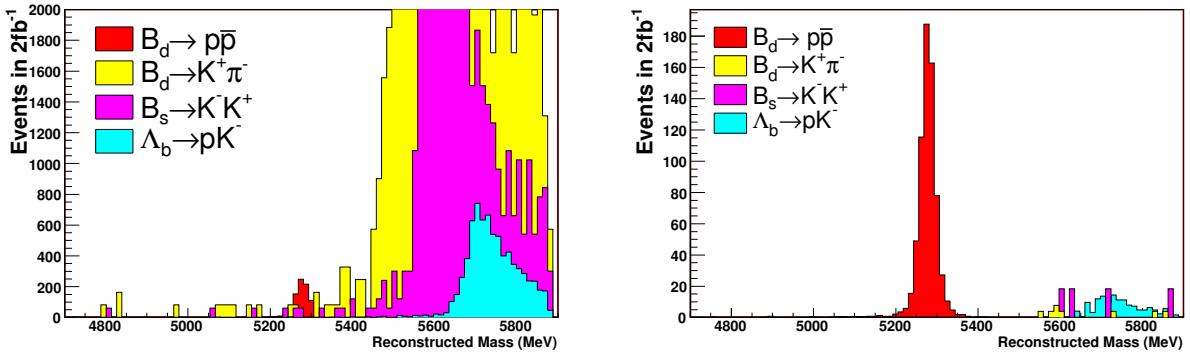

Figure 2: Reconstructed mass distributions before (left) and after (right) PID cuts for $B^0 \to p\bar{p}$ (red), $B^0 \to K^+\pi^-$ (yellow), $B_s \to K^+K^-$ (purple) and $\Lambda_b \to pK^-$ (cyan) events.

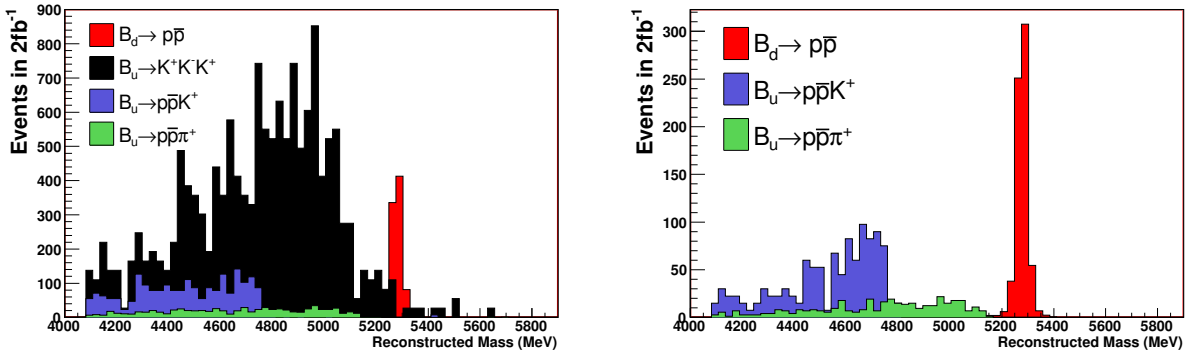

Figure 3: Reconstructed mass distributions before (left) and after (right) PID cuts for $B^0 \to p\bar{p}$ (red), $B^+ \to K^+K^-K^+$ (black) , $B^+ \to p\bar{p}K^+$ (violet) and $B^+ \to p\bar{p}\pi^+$ (dark green) events.

From Figs. 2 and 3 it is clear that a mass window of 50 MeV around the B^0 mass removes almost all of the background from the $B \to h^+h'^-$ channels and some of the $B \to hhh$ channels, even before PID cuts being applied. However, Figs. 4 and 5 show that this is not the case for the remaining $B \to hhh$ channels where PID cuts are crucial in reducing the background level.

Figs. 6 and 7 illustrate why the PID cuts are so effective against the specific background. Fig. 6 compares the distributions of DLL$(p-\pi)$ for true protons from $B^0 \to p\bar{p}$ and true pions from $B^0 \to \pi^+\pi^-\pi^0$. There is excellent separation: the cut at DLL$(p-\pi) = 5$ removes almost all of the $B^0 \to \pi^+\pi^-\pi^0$ events whilst having very high signal efficiency. Fig. 7 compares the distributions of DLL$(p-K)$ for true protons from $B^0 \to p\bar{p}$ and true kaons from $B^+ \to \pi^+\pi^-K^+$. Again, there is very good separation: the cut at DLL$(p-K) = 0$ removes a large majority of the background with minimal effect on the signal. The PID cuts are in fact even more powerful than Figs. 6 and 7 at first suggest, because they are applied to both daughter particles, so that an event without a true proton must have both daughters in the tail of the DLL distribution, which is very unlikely. Of course

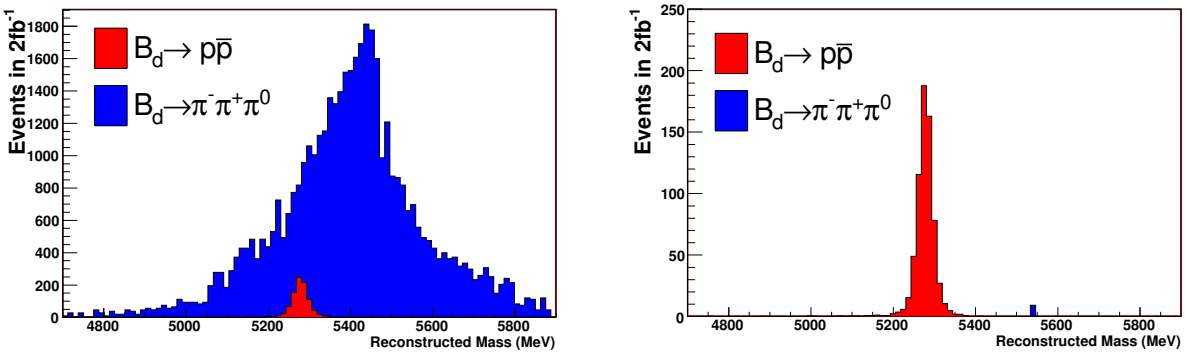

Figure 4: Reconstructed mass distributions before (left) and after (right) PID cuts for $B^0 \to p\bar{p}$ (red) and $B^0 \to \pi^+\pi^-\pi^0$ (blue) events.

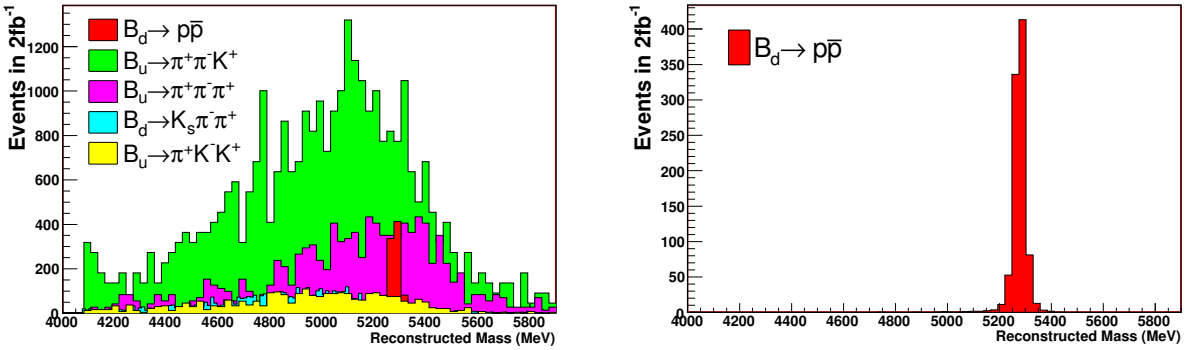

Figure 5: Reconstructed mass distributions before (left) and after (right) PID cuts for $B^0 \to p\bar{p}$ (red), $B^+ \to \pi^+\pi^-K^+$ (green), $B^+ \to \pi^+\pi^-\pi^+$ (pink), $B^0 \to K_s\pi^-\pi^+$ (cyan) and $B^+ \to \pi^+K^-K^+$ (yellow) events.

a few specific backgrounds ($\Lambda_b \to pK^-$, $B^+ \to p\bar{p}K^+$ and $B^+ \to p\bar{p}\pi^+$) do contain a true proton, but it has been shown that the invariant mass distributions for these channels do not overlap with the signal peak. To summarise, it is clear that the $B \to hhh$ background which is present in the signal mass region can be very effectively reduced using PID information.

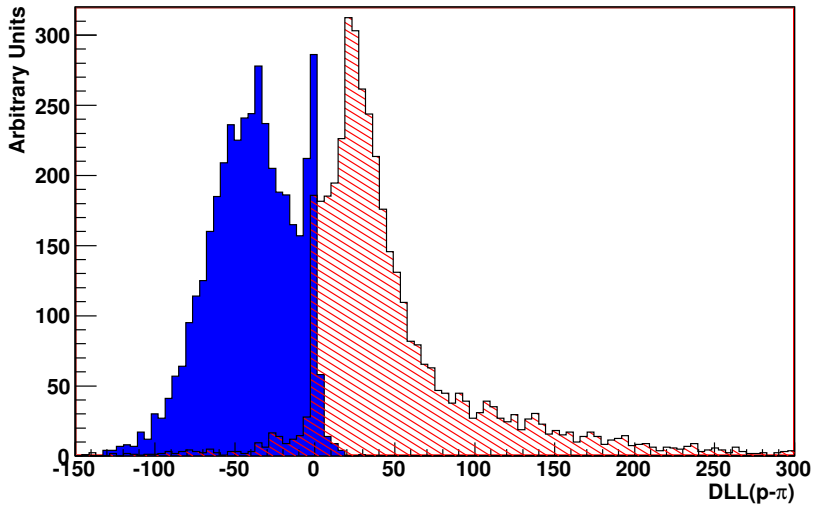

Figure 6: Distributions of DLL($p - \pi$) for $B^0 \to p\bar{p}$ (red, hatched) and $B^0 \to \pi^+\pi^-\pi^0$ (blue) events.

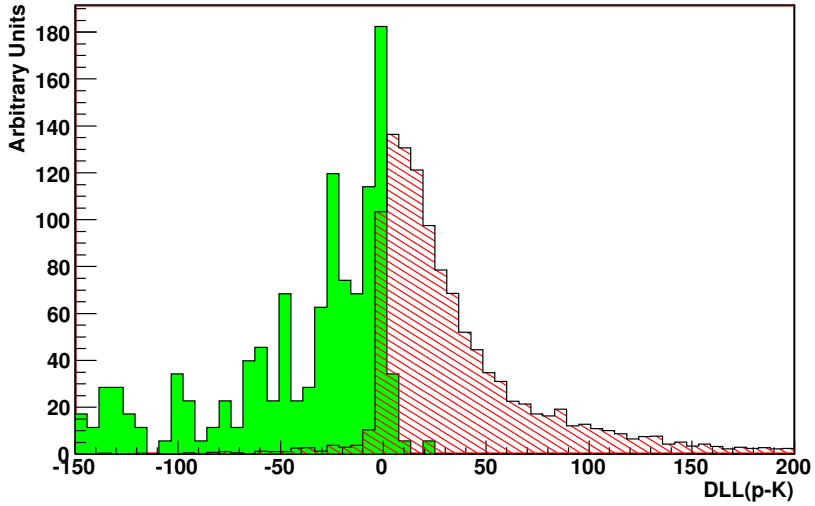

Figure 7: Distributions of DLL$(p-K)$ for $B^0 \to p\bar{p}$ (red, hatched) and $B^+ \to \pi^+\pi^-K^+$ (green) events.

Finally, the effectiveness of the cut on the quality of the track fit is illustrated in Fig. 8, which compares the track $\chi^2/n_{\rm DoF}$ distributions from signal tracks with that for ghost tracks from $b\bar{b}$ inclusive events. Note that the $b\bar{b}$ inclusive events in Fig. 8 have only been passed through a very loose preselection, so that enough $b\bar{b}$ inclusive events survive to make the $\chi^2/n_{\rm DoF}$ distribution for ghosts tracks apparent.

A cut of $\chi^2/n_{\rm DoF} < 3$ removes many ghost tracks, while having almost no effect on signal tracks. This cut also removes the few $b\bar{b}$ inclusive events which survive the other selection cuts.

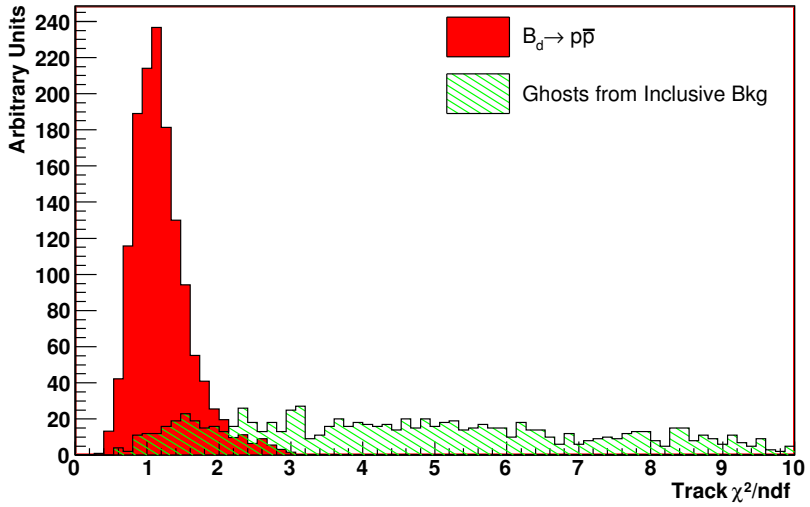

Figure 8: Distributions of track $\chi^2/n_{\rm DoF}$ for $B^0 \to p\bar{p}$ (red) and $b\bar{b}$ inclusive (green, hatched) events. See text for details.

5 LHCb Sensitivity to $B^0 \to p\bar{p}$

5.1 Selection Performance

The standard $B \to h^+h'^-$ selection was run on simulated data samples of signal and specific background events, with a typical size of order 100,000 events per channel. An inclusive $b\bar{b}$ sample consisting of 980,000 stripped

events [1] was used, corresponding to around 27 million unstripped events. Finally, around 5.5 million minimum bias events, which passed the first-level (L0) trigger, were used. The physics analysis program `DaVinci` [14] version `v19r14` was employed.

A mass window of 50 MeV around the nominal B^0 mass was applied for the signal and specific background sources, while for the $b\bar{b}$ inclusive and minimum bias samples the mass window was widened to 600 MeV, to increase statistics. Their yields were later scaled down by a factor of 12 to account for this widened window.

The selection described in Sec. 3 is found to have an efficiency ($\epsilon_{\rm sel}$) of 9.8% on signal. No background event of any category was found to survive this selection. The specific background events are rejected mainly by a combination of PID and invariant mass cuts, whilst the $b\bar{b}$ inclusive and minimum bias events are rejected mainly by the standard selection cuts such as impact parameter significances and transverse momentum p_T cuts.

Given that no background events are selected, an upper limit on the selection efficiency $\epsilon_{\rm sel}$ at 90% C.L. can be found using the Feldman-Cousins statistical approach [15]. For zero selected events, it attributes an upper limit on the number of selected events of 2.44 at 90% C.L., which can be converted into a 90% C.L. upper limit on $\epsilon_{\rm sel}$.

Table 4 gives the size of each background sample [2], and the upper limit on $\epsilon_{\rm sel}$ for each. It also gives the geometrical efficiency ($\epsilon_{\rm geo}$) of each channel, *i.e.* the percentage of events that pass the generator level cut which requires that all decay products of the signal B lie within the LHCb acceptance [3]. The branching ratio (B.R.) of each channel is also given. Note that for all but one channel, the branching ratio used is the mean value given in the Particle Data Group 2008 review [16]. The exception is $\Lambda_b \to pK^-$, the branching ratio of which was very recently measured [17] for the first time by the CDF Collaboration.

Decay Channel	Size of Sample	Upper Limit on $\epsilon_{\rm sel}$	$\epsilon_{\rm geo}$ (%)	Branching Ratio
$B^0 \to \pi^+\pi^-\pi^0$	139,322	1.8×10^{-5}	18.3	2.5×10^{-5}
$B^0 \to K_s\pi^-\pi^+$	457,135	5.3×10^{-6}	21.2	2.2×10^{-5}
$B^+ \to \pi^+\pi^-\pi^+$	61,138	4.0×10^{-5}	17.9	1.6×10^{-5}
$B^+ \to \pi^+\pi^-K^+$	65,110	3.7×10^{-5}	18.3	5.5×10^{-5}
$B^+ \to \pi^+K^-K^+$	63,141	3.9×10^{-5}	18.7	5.0×10^{-6}
$B^+ \to p\bar{p}\pi^+$	68,078	3.6×10^{-5}	20.0	1.6×10^{-6}
$B^+ \to p\bar{p}K^+$	46,737	5.2×10^{-5}	20.6	5.9×10^{-6}
$B^+ \to K^+K^-K^+$	67,118	3.6×10^{-5}	19.3	3.4×10^{-5}
$B^0 \to K^+\pi^-$	296,700	8.2×10^{-6}	20.2	1.9×10^{-5}
$B_s \to K^+K^-$	99,048	2.5×10^{-5}	34.6	3.3×10^{-5}
$\Lambda_b \to pK^-$	64,579	3.8×10^{-5}	21.1	5.0×10^{-6}
Inclusive $b\bar{b}$	26.94M	9.1×10^{-8}	43.7	n/a
L0-yes minimum bias	5.55M	4.4×10^{-7}	n/a	n/a

Table 4: Channel-specific values used to evaluate signal and background yields. Limits shown correspond to a 90% confidence level upper limit.

5.2 Signal and Background Yields

The yield in 2 fb^{-1} of integrated luminosity (defined as a "nominal LHCb year", amounting to 10^7 s of data taking at a nominal average luminosity) for signal and for a specific B background is given by

$$\text{Yield} = \epsilon_{\rm sel} \times \epsilon_{\rm trig} \times \epsilon_{\rm geo} \times f_B \times \text{B.R.} \times \int \mathscr{L} dt \times 2 \times \sigma_{b\bar{b}}. \quad (1)$$

Here, $\epsilon_{\rm trig}$ is the efficiency of the LHCb trigger on events of that type which have passed the selection, f_B is the probability for a b quark to form the relevant B hadron, $\mathscr{L}$ is the average luminosity at the LHCb interaction point, and $\sigma_{b\bar{b}}$ is the beauty cross section at 14 TeV centre-of-mass energy. The factor of 2 accounts for the production of both a b and a $\bar{b}$.

The yields for $b\bar{b}$ inclusive background and minimum bias background are, respectively,

[1] Stripped events are events passing at least one of a set of looser pre-selection cuts typically designed for specific B-decays.
[2] When stripped samples were used, the stripping efficiency has been accounted for to give an effective sample size.
[3] The $B_s \to K^+K^-$ sample uses a looser cut, which requires instead that the signal B lies within the LHCb acceptance.

$$\text{Yield}_{b\bar{b}} = \epsilon_{\text{sel}} \times \epsilon_{\text{trig}} \times \epsilon_{\text{geo}} \times \int \mathscr{L} dt \times \sigma_{b\bar{b}} \times \frac{1}{12} \tag{2}$$

and

$$\text{Yield}_{\text{MB}} = \epsilon_{\text{sel}} \times \epsilon_{\text{trig}} \times \text{Rate}_{\text{L0}} \times \text{Time}_{2\text{fb}^{-1}} \times \frac{1}{12}, \tag{3}$$

where we recall that these yields are scaled down by a factor 12 to account for the wide mass window used in their selection. In Eq. 3, Rate_{L0} is the output rate of the L0 trigger, and $\text{Time}_{2\text{fb}^{-1}}$ is the time taken to accumulate 2 fb^{-1} of data at the nominal LHCb luminosity. Values for these quantities, along with $\sigma_{b\bar{b}}$ and f_B, are given in Tab. 5. Note that the $\sigma_{b\bar{b}}$ value is a working assumption, based on theoretical predictions from QCD.

The efficiency of the trigger with respect to selected $B \to h^+h'^-$ events has been studied in [13]. It was found that for the main $B \to h^+h'^-$ channels, ϵ_{trig} was always in the range [35%, 38%]. Although the precision was limited by available statistics in the simulation of background events, ϵ_{trig} for the backgrounds (both physics backgrounds like $B \to hhh$ and $b\bar{b}$ inclusive background) was found to be broadly similar to ϵ_{trig} for the signals. This is expected, as the background events that have passed the selection are in some sense "signal-like". Hence here a conservative assumption is made taking $\epsilon_{\text{trig}} = 36\%$ for signal, specific background and $b\bar{b}$ inclusive background. The value for the L0-yes minimum bias sample is higher (68%) as these events have already passed the L0 trigger, which has an efficiency of around 53% on the selected events.

Parameter	Value used
Luminosity $\mathscr{L}$	$2\times10^{32}\text{cm}^{-2}\text{s}^{-1}$
$\sigma_{b\bar{b}}$	500 μb
Rate_{L0}	10^6 Hz
$\text{Time}_{2\text{fb}^{-1}}$	10^7 s
$f_B(B^0)$	0.40±0.01
$f_B(B^+)$	0.40±0.01
$f_B(B_s)$	0.11±0.01
$f_B(\Lambda_b)$	0.07±0.02

Table 5: General constants used to evaluate signal and background yields. The values for f_B are taken from [16].

The signal yield per 2 fb^{-1} was calculated assuming the current experimental limit of 1.1×10^{-7} for the $B^0 \to p\bar{p}$ branching ratio; it is found to be 678 events per 2 fb^{-1}. The values used to calculate the signal yields are given in Tab. 6. Table 7 shows the upper limits on the background yields and the resulting background-to-signal ratios. Each upper limit is calculated using the relevant yield equation as given above, taking the relevant upper limit on ϵ_{sel} from Tab. 4.

Table 6: Values used to evaluate signal yield.

Decay channel	Size of sample	ϵ_{sel} (%)	ϵ_{geo} (%)	Branching ratio	2 fb^{-1} yield
$B^0 \to p\bar{p}$	46707	9.8	21.9	1.1×10^{-7}	678

The constraint placed on the minimum bias yield is severely limited by the quantity of available simulated minimum bias events. It is assumed in what follows that the amount of minimum bias events passing the trigger and the final offline selection will be negligible. This assumption is expected to be valid because selection cuts which supress background from B decays should be even more effective against background from charm and lighter quarks. As a consequence, any possible background contribution from minimum bias events will hereafter be neglected.

With this condition, the upper limit (at 90% confidence level) on the total background-to-signal ratio is:

$$\begin{aligned} B/S_{\text{total}} &= B/S_{B\to h^+h'^-} + B/S_{B\to hhh} + B/S_{b\bar{b}\text{inclusive}} \\ &< 0.05 + 0.40 + 1.75 \qquad \text{(at 90\% C.L.)} \\ &= 2.20 \end{aligned}$$

Decay Channel	Upper limit on 2 fb^{-1} yield	Upper limit on B/S
$B^0 \to \pi^+\pi^-\pi^0$	23	0.034
$B^0 \to K_s\pi^-\pi^+$	7	0.011
$B^+ \to \pi^+\pi^-\pi^+$	33	0.048
$B^+ \to \pi^+\pi^-K^+$	109	0.160
$B^+ \to \pi^+K^-K^+$	10	0.015
$B^+ \to K^+K^-K^+$	69	0.101
$B^+ \to p\bar{p}\pi^+$	3	0.005
$B^+ \to p\bar{p}K^+$	18	0.027
$B^0 \to K^+\pi^-$	9	0.013
$B_s \to K^+K^-$	22	0.033
$\Lambda_b \to pK^-$	2	0.003
Inclusive $b\bar{b}$	1,188	1.75
Minimum Bias	249,129	367.4

Table 7: Upper limits on background yields and resulting B/S values. Limits correspond to a 90% confidence level.

Note that there are two conservative assumptions used in the calculation of this upper limit. Firstly, simply summing a number of 90% confidence levels from different sources overestimates the total upper limit. Secondly, it is assumed that there is no overlap between the inclusive and specific background sources.

5.3 Signal Significance

In the following calculation of the expected signal significance, the upper limit on the background-to-signal ratio calculated above is conservatively taken as the central value. The significance of the $B^0 \to p\bar{p}$ signal can be expressed as a function of integrated luminosity and its (currently unknown) branching fraction. The significance is defined as

$$\text{Significance} = \frac{\mathrm{N_{sig}}}{\sqrt{\mathrm{N_{sig}} + \mathrm{N_{bkg}}}} , \tag{4}$$

where $\mathrm{N_{sig(bkg)}}$ is the number of signal (background) events.

Figure 9 shows, for four possible values for the branching ratio of $B^0 \to p\bar{p}$, how the significance evolves with integrated luminosity. If the true branching ratio is close to the current experimental upper limit, a discovery at the 5σ level can be made with early LHCb data. Taking the current upper limit, a 5σ significance is achieved with of order 0.25 fb^{-1} of data. Even if the true branching ratio is a factor of 5 below the current limit, which would contradict all existing theoretical predictions, LHCb can make a discovery with 5.3 fb^{-1}.

5.4 Prospects for 2010

The initial physics run of the LHC, starting in late 2009 and finishing in late 2010, will feature a lower than nominal centre-of-mass energy. In this section the discovery prospects for $B^0 \to p\bar{p}$ in 2010 are examined, assuming a centre-of-mass energy of $E_{\mathrm{CM}} = 10$ TeV.

The lower E_{CM} value will lower the beauty cross section $\sigma_{b\bar{b}}$. The Monte Carlo-based program Pythia [18], used to simulate high-energy pp collisions, predicts (version 6.2) that at $E_{\mathrm{CM}} = 10$ TeV, $\sigma_{b\bar{b}}$ will be a factor $\simeq$0.77 less than at $E_{\mathrm{CM}} = 14$ TeV. Hence, assuming that the reconstruction and trigger performances are similar at $E_{\mathrm{CM}} = 10$ TeV, the signal and background[4)] yields in Tab. 7 will all be scaled down by the same factor. Hence the background-to-signal ratio for a given $B^0 \to p\bar{p}$ branching ratio will not change. However the signal significance will change as it is not a linear function of the signal and background yields.

The signal significance for $B^0 \to p\bar{p}$ as a function of integrated luminosity for data taken with $E_{\mathrm{CM}} = 10$ TeV is shown in Fig 10.

It can be seen that 0.32 fb^{-1} of data at $E_{\mathrm{CM}} = 10$ TeV is required to achieve 5σ significance, assuming a branching ratio close to the current experimental limit. Such an amount of data is unlikely to be collected in the initial physics run of the LHC.

However it should be recalled that the background-to-signal ratio assumed in Fig. 10 is the upper limit at 90% confidence level. Should the background-to-signal ratio on data be significantly below this upper limit,

[4)] The minimum bias yield will not scale with the same factor, but since minimum bias background was neglected this is not relevant here.

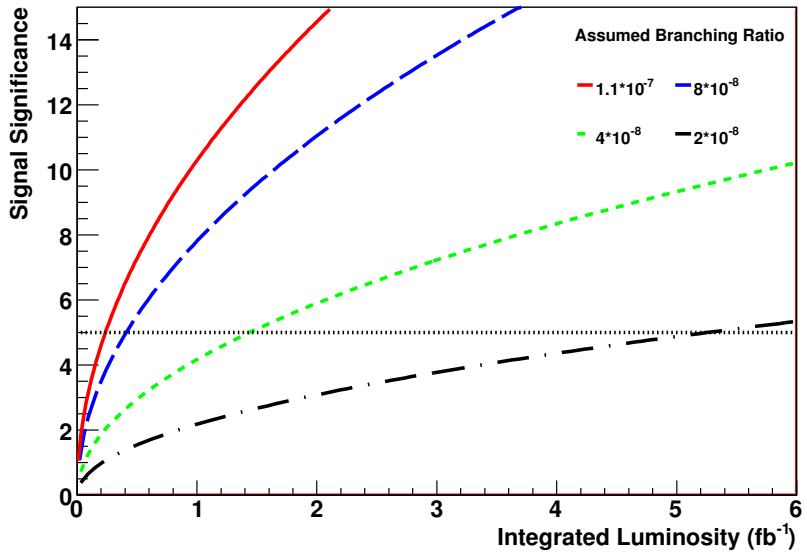

Figure 9: Significance of the $B^0 \to p\bar{p}$ signal as a function of integrated luminosity, assuming a centre-of-mass energy of $E_{\rm CM} = 14$ TeV. Each curve assumes a different $B^0 \to p\bar{p}$ branching ratio: 1.1×10^{-7} (red, solid), 8×10^{-8} (blue, long dashes), 4×10^{-8} (green, short dashes) and 2×10^{-8} (black, dash-dot).

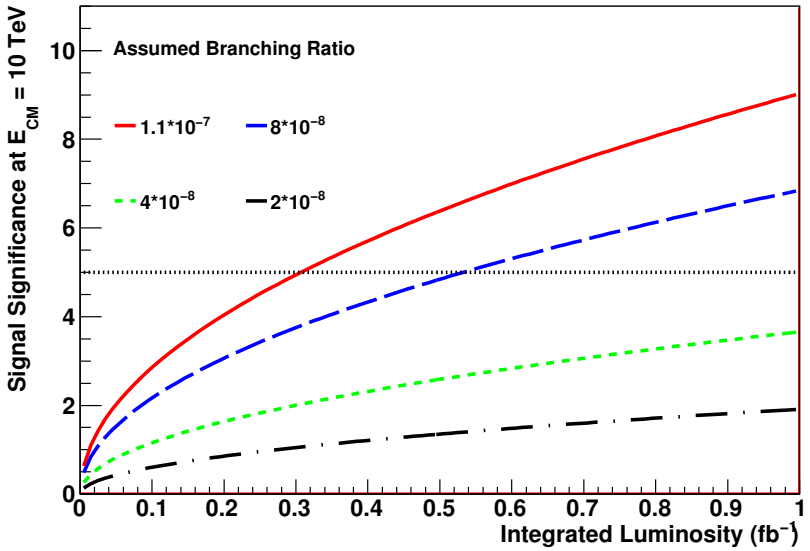

Figure 10: Significance of the $B^0 \to p\bar{p}$ signal as a function of integrated luminosity, assuming $E_{\rm CM} = 10$ TeV. Each curve assumes a different $B^0 \to p\bar{p}$ branching ratio: 1.1×10^{-7} (red, solid), 8×10^{-8} (blue, long dashes), 4×10^{-8} (green, short dashes) and 2×10^{-8} (black, dash-dot).

an observation may still be made in the initial physics run. For illustration, assuming that 0.2 fb^{-1} of data are collected at $E_{\rm CM} = 10$ TeV (this is considered feasible for the initial physics run), and again assuming a branching ratio close to the current experimental limit, a background-to-signal ratio of 1.09 would lead to a 5σ discovery of $B^0 \to p\bar{p}$.

6 Measurement of the $B^0 \to p\bar{p}$ Branching Ratio

Once a 5σ signal for $B^0 \to p\bar{p}$ has been observed, its branching ratio can be determined. This can be done by normalising the branching ratio to that of $B^0 \to K^+\pi^-$, which is the $B \to h^+h^{'-}$ channel with the highest

branching ratio and smallest experimental error. Its branching ratio has been precisely measured by the B-factories to be $(1.94 \pm 0.06) \times 10^{-5}$. The branching ratio for $B^0 \to p\bar{p}$ can be obtained from this as follows.

Firstly, the yield in each channel will be measured. This is done by fitting to the peak in the invariant mass distribution after all relevant cuts have been applied, taking the invariant mass distributions of the various backgrounds into account. For $B^0 \to K^+\pi^-$, the fit to the invariant mass distribution will be done simultaneously with the other main $B \to h^+h^{'-}$ channels, as their distributions overlap significantly (the fitting method is described in [13]). PID cuts will not have been applied at this stage. For $B^0 \to p\bar{p}$ the only other signal mass distribution in that region will be $B_s \to p\bar{p}$, which is expected to make a negligible contribution to the mass peak (see Sec. 8.1). PID cuts will need to be applied before this fit can be made, as otherwise the signal will be swamped by specific backgrounds (see Sec. 4.2) and $b\bar{b}$ inclusive background.

Then the efficiencies of the trigger and selection need to be taken into account. The efficiency $\epsilon_{\rm sel}$ of a full offline selection for a $B \to h^+h^{'-}$ channel can be broken down using $\epsilon_{\rm sel} = \epsilon_{\rm top/kin} \times \epsilon_{\rm PID}$, where $\epsilon_{\rm top/kin}$ accounts for the topological and kinematic cuts and $\epsilon_{\rm PID}$ accounts for the PID cuts. Then $\epsilon_{\rm top/kin}$ should be almost the same for $B^0 \to K^+\pi^-$ and $B^0 \to p\bar{p}$, while $\epsilon_{\rm PID}$ will be different. However $\epsilon_{\rm PID}$ can be estimated using control channels which will be used to calibrate the PID performance.

For calibration of the proton PID, the decay $\Lambda \to p\pi^-$ is used [19]. Studies aiming to calibrate the kaon and pion PID using $D^{*+} \to D^0(K\pi)\pi^+$ decays [13] have shown very promising results, hence the proton PID calibration can also be expected to perform well, especially considering the higher production rate of Λ with respect to D^{*+}. Hence the estimation of $\epsilon_{\rm PID}$ should not be a major source of systematic error.

The trigger efficiency is expected to be very similar in the two channels (assuming that the trigger mass window is wide enough, see Sec. 7), as they will have to pass the same cuts there. Finally, the ratio of the geometrical efficiencies for the two channels can be accurately estimated from simulation.

Under these assumptions, Eqn. 1 can be used to obtain an expression for the $B^0 \to p\bar{p}$ branching ratio ($\epsilon_{\rm PID}$ does not appear for $B^0 \to K^+\pi^-$ as the $B^0 \to K^+\pi^-$ yield will be calculated before PID cuts are applied):

$$\mathrm{BR}(B^0 \to p\bar{p}) = \mathrm{BR}(B^0 \to K^+\pi^-) \times \frac{\mathrm{Yield}_{p\bar{p}} \times \epsilon_{\mathrm{geo}(K\pi)}}{\mathrm{Yield}_{K\pi} \times \epsilon_{\mathrm{PID}(p\bar{p})} \times \epsilon_{\mathrm{geo}(p\bar{p})}} \tag{5}$$

All of the terms on the right-hand side of Eqn. 5 can be obtained as described above to give a value for $\mathrm{BR}(B^0 \to p\bar{p})$.

7 Trigger Mass Window

In the high-level trigger selection of $B \to h^+h^{'-}$ channels, a pion mass hypothesis is assumed for all B-daughters. As a result, the reconstructed mass for a $B^0 \to p\bar{p}$ event will be far below the nominal B^0 mass (see Fig. 11). It follows that in order to select $B^0 \to p\bar{p}$ events in the trigger, the mass window must extend at least $\backsimeq$500 MeV below the nominal B^0 mass. A mass window of $m_{B^0} \pm 600$ MeV for example would select 87% of signal events. Having the trigger mass window similar to this would, as well as losing some signal events, also add an extra systematic effect in the calculation of the $B^0 \to p\bar{p}$ branching ratio, as the percentage of events lost due to the mass window would have to be estimated using a Monte Carlo simulation of the invariant mass shape. Hence, from the point of view of $B^0 \to p\bar{p}$, the best mass window for the trigger to use would be one which started far below the $B^0 \to p\bar{p}$ peak – a window lower limit around 4400 MeV.

8 Other Two-Body Charmless Baryonic B Decays

8.1 Prospects for the Observation of $B_s \to p\bar{p}$

The decay $B_s \to p\bar{p}$ is expected to be rather suppressed relative to $B^0 \to p\bar{p}$; in the Standard Model it can only occur via annihilation diagrams, given that none of the quarks in the final state are those of the initial B_s meson. Despite the lack of any firm theoretical predictions, it is legitimate to search for this rare mode given its identical final state. LHCb has the potential to improve the present experimental branching ratio upper limit – $\approx 5.9 \times 10^{-5}$ – by several orders of magnitude.

Figure 12 shows the mass distributions of $B^0 \to p\bar{p}$ and $B_s \to p\bar{p}$ events as expected after applying the full selection (including PID cuts) to 2 fb^{-1} of data, in the absence of background. Note that the core width of the mass distribution is 17 MeV. The assumed branching ratios are 1.1×10^{-7} for $B^0 \to p\bar{p}$ and 1.1×10^{-8} for $B_s \to p\bar{p}$. Far fewer $B_s \to p\bar{p}$ events are present due to the lower assumed branching ratio, and the fact that $f_B(B^0)/f_B(B_s) \approx 4$.

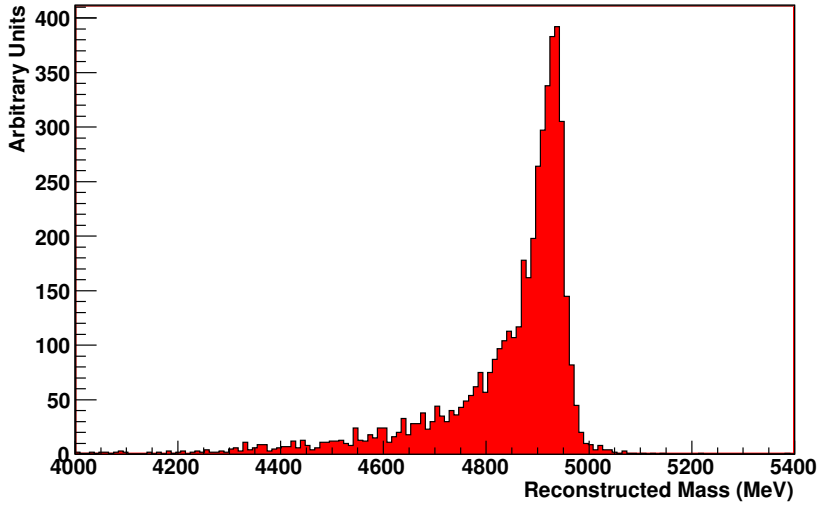

Figure 11: Reconstructed mass distribution for offline selected $B^0 \to p\bar{p}$ events taking the pion mass hypothesis for the B-daughters.

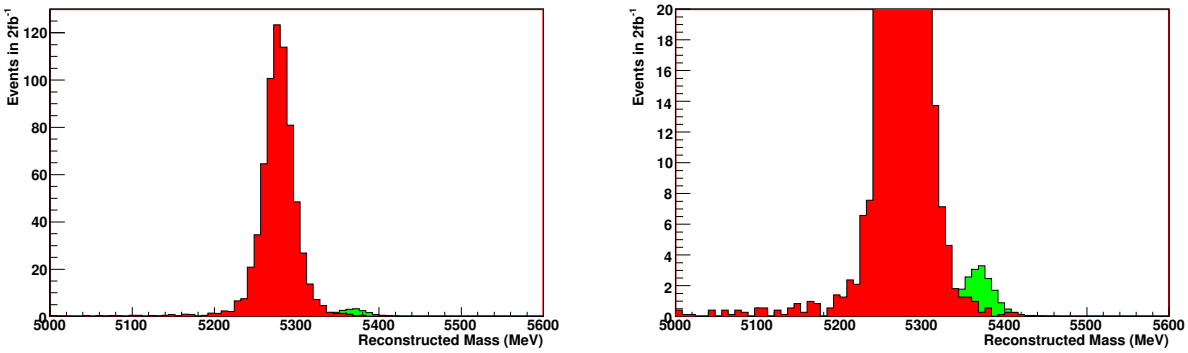

Figure 12: Reconstructed mass distributions for $B^0 \to p\bar{p}$ (red) and $B_s \to p\bar{p}$ (green) events. The right-hand plot is a detail of the left-hand plot.

Figure 12 illustrates that the much larger $B^0 \to p\bar{p}$ peak will form a significant "background" to $B_s \to p\bar{p}$, and will become more significant if the mass resolution in data is poorer than in the simulation. Combined with the presence of the background sources described in Sec. 4, this means that a significant amount of data will be required in order to observe the $B_s \to p\bar{p}$ mass peak.

8.2 Prospects for Decays Involving a Λ

Other two-body charmless baryonic B decays which can be reconstructed by LHCb include $B^+ \to p\bar{\Lambda}$ and $B^0 \to \Lambda\bar{\Lambda}$, in cases where the Λ decays via $\Lambda \to p\pi^-$. As with $B^0 \to p\bar{p}$, theoretical calculations of their branching fractions are subject to debate, with predictions differing by up to an order of magnitude, *cf.* Tab. 1. The dominant diagram contributing to $B^+ \to p\bar{\Lambda}$ is expected to be the gluonic penguin shown in Fig. 13. This is in constrast to $B^0 \to p\bar{p}$, where the tree process is expected to dominate.

LHCb can also look for the $B_s \to \Lambda\bar{\Lambda}$ decay. Whereas $B_s \to p\bar{p}$ should be rather suppressed compared to $B^0 \to p\bar{p}$ (see Sec. 8.1), $B_s \to \Lambda\bar{\Lambda}$ could have a relatively large branching ratio of the same order of that of $B^+ \to p\bar{\Lambda}$, as the penguin diagrams mediating these processes are identical apart from their spectator quarks (which are related by a V-spin transformation).

It is worth mentioning that the latest upper limit measurements from the Belle Collaboration, shown on Tab. 2, are close to excluding all theoretical predictions. Moreover, a discovery of the decay $B^0 \to \Lambda\bar{\Lambda}$ would crucially constrain the MIT bag model calculation approach in the pole model.

The selection efficiency for such decays will depend crucially on the efficiency for reconstructing Λ baryons, a detailed analysis of which is left as future work. However it should be noted that reconstruction of Λ baryons

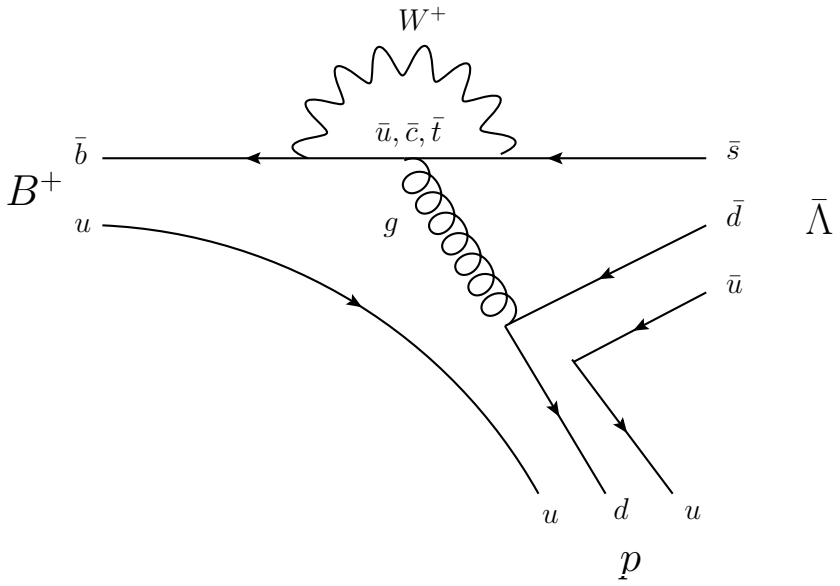

Figure 13: Feynman diagram for the penguin process contributing to $B^+ \to p\bar{\Lambda}$.

from B decays has been shown [20, 21] to be viable for LHCb. In addition the presence of two protons in the final state will enable excellent suppression of background through PID cuts (compare Sec. 4.2). Hence observation of $B^+ \to p\bar{\Lambda}$ and $B_s \to \Lambda\bar{\Lambda}$ may be feasible, depending on the value of their branching ratios.

9 Conclusions

The potential of LHCb to discover the rare decay $B^0 \to p\bar{p}$ has been explored. It is found that around 0.25 fb^{-1} of data (at $E_{CM} = 14$ TeV) will be required for a 5σ discovery, assuming that the $B^0 \to p\bar{p}$ branching fraction is close to the current experimental upper limit. Even if the true branching fraction is a factor of 5 lower than the present upper limit, a discovery can be made with about 5 fb^{-1} of data.

Observations of other charmless two-body baryonic B decays may also be possible, but these require further study.

Acknowledgements

We would like to thank George Hou, who pointed out the interesting experimental and theoretical status of two-body charmless baryonic B decays, and its suitability for a study by LHCb. We also thank Chris Parkes for support and enthusiasm in this study.

References

[1] Y.-T. Tsai, P. Chang, *et al.* (Belle Collaboration), *Search for $B^0 \to p\bar{p}$, $B^0 \to \Lambda\bar{\Lambda}$ and $B^+ \to p\bar{\Lambda}$ at Belle*, Phys. Rev. D75, 111101 (2007).

[2] B. Aubert *et al.* (BaBar Collaboration), Phys. Rev. D69, 091503 (2004).

[3] T. E. Coan *et al.* (CLEO Collaboration), *Search for exclusive rare baryonic decays of B mesons*, Phys. Rev. D59, 111101 (1999).

[4] LHCb Collaboration, *The LHCb Detector at the LHC*, 2008 JINST 3 S08005 (2008); `http://www.iop.org/EJ/journal/-page=extra.lhc/jinst`.

[5] LHCb Collaboration, *LHCb Reoptimized Detector Design and Performance*, CERN LHCC 2003-030.

[6] V. Chernyak and I. Zhitnitsky, Nucl. Phys. B345, 137 (1990).

[7] P. Ball and H.G. Dosch, Z. Phys. C51, 445 (1991).

[8] M. Jarfi *et al.*, Phys. Rev. D43, 1599 (1991); Phys. Lett. B237, 513 (1990).

[9] H.Y. Cheng and K.C. Yang, Phys. Rev. D66 014020 (2002).

[10] Y. Kubota *et al.* (CLEO Collaboration), Nucl. Instr. Meth. A 320, 66 (1992).

[11] B. Aubert *et al.* (BaBar Collaboration), Nucl. Instr. Meth. A 479, 1 (2002).

[12] A. Abashian *et al.* (Belle Collaboration), Nucl. Instr. Meth. A 479, 117 (2002).

[13] A. Bates *et al.*, *Road map for charmless charged two-body B decays at LHCb*, LHCb Note in preparation.

[14] `http://lhcb-release-area.web.cern.ch/LHCb-release-area/DOC/davinci/`.

[15] G. Feldman and R. Cousins, *A Unified approach to the classical statistical analysis of small signals*, Phys. Rev. D57, 3873 (1998).

[16] C. Amsler *et al.*, *Review of Particle Physics*, Phys. Lett. B667, 1 (2008).

[17] The CDF Collaboration, *Measurement of CP-violating asymmetries and of branching fractions of $\Lambda_b^0 \to p\pi^-$ and $\Lambda_b^0 \to pK^-$ decays* , CDF Note 9092; `http://www-cdf.fnal.gov/physics/new/bottom/071018.blessed-ACP_Lambdab_ph/`.

[18] Pythia Homepage. `http://home.thep.lu.se/~torbjorn/Pythia.html`

[19] B. Popovici and S. Stoica, *Calibration of LHCb RICH Detectors with $\Lambda \to p\pi^-$ Decay using Data*, Presented at *Physics at LHC - 2008*, Split, Croatia, 29th September - 4th October 2008; CERN-Poster-2008-047, `http://cdsweb.cern.ch/record/1133609`.

[20] F. Legger, *Reconstruction of the decays $\Lambda_b^0 \to \Lambda(1115)\gamma$ and $\Lambda_b^0 \to \Lambda(1670)\gamma$ at LHCb*, LHCb 2006-012, 18th December 2006.

[21] F. Legger, *Polarized radiative Λ_b^0 decays at LHCb*, LHCb 2006-013, 18th December 2006.